

## Magnetoacoustic Attenuation in High-Field Superconductors

Y. SHAPIRA AND L. J. NEURINGER

*National Magnet Laboratory,\* Massachusetts Institute of Technology, Cambridge, Massachusetts*

(Received 11 August 1966)

A phenomenological model for the magnetic-field variation of the ultrasonic attenuation in the mixed and normal states of a high-field superconductor is developed. It is shown that the attenuation in the mixed state is related to the motion of the Abrikosov flux lines and is greatly affected by the strength of the pinning forces which inhibit this motion. The pinning forces are characterized by the "depinning frequency"  $\omega_0$ . At frequencies well above  $\omega_0$  the attenuation is directly related to the dc flow resistivity. A method for determining  $\omega_0$ , and hence the strength of the pinning forces, from ultrasonic data is outlined. Ultrasonic-attenuation measurements were carried out on five different high-field superconducting alloys, viz., annealed Nb-25 at.% Zr, Nb-32 at.% Ti, V-42 at.% Ti, V-21 at.% Ti, and unannealed Nb-25 at.% Zr. These measurements were performed at liquid-helium temperatures and in steady magnetic fields up to 100 kG. Shear and longitudinal sound waves, with frequencies ranging from 8 to 56 Mc/sec, were used. The data are compared in detail with the predictions of the phenomenological model. It is found that in all cases there is good agreement between experiment and theory. In particular, it is shown that estimates of the depinning frequency obtained from the ultrasonic data agree with those derived from critical-current measurements carried out on the same materials.

### I. INTRODUCTION

**H**IGH-field superconducting alloys are a new class of materials whose properties have been investigated in the past few years. Interest in these materials stems from the rich variety of physical phenomena which they exhibit, as well as from their technical applications, notably in the construction of superconducting magnets. Recently, there have been several investigations of the response of high-field superconductors, in the mixed state, to electric fields varying in frequency from dc<sup>1</sup> through the rf<sup>2</sup> to the microwave region.<sup>3</sup> It was found that the response to these perturbations can be understood by considering the motion of the Abrikosov flux lines (flux flow) and the strong influence of the pinning forces on this motion. For weak electric fields and at low frequencies the pinning forces inhibit flux flow. On the other hand, at very high frequencies the motion of the flux lines is virtually unaffected by the pinning forces. As a consequence, the low-frequency response of a high-field superconductor, in the mixed state, is qualitatively different from its response at high frequencies. The transition between these two frequency regimes occurs generally at  $\sim 0.1$ –100 Mc/sec. In this intermediate frequency range the response of the superconductor is sensitive to the strength of the pinning forces. As a result, measurements at radio frequencies should be very useful in studying the pinning forces. Ultrasonic waves, in the commonly used radio-frequency range, provide therefore a means of probing the *bulk* properties of the

mixed state, especially flux flow and its dependence on the pinning forces.

The use of ultrasonic attenuation measurements in the study of low-field type-I superconductors has been widespread and has yielded considerable information about the BCS energy gap and its anisotropy.<sup>4</sup> One might expect that ultrasonic techniques will also become useful in the elucidation of the properties of high-field superconductors. To achieve this end it is necessary to have a theory which relates the results of ultrasonic measurements to the basic properties of the high-field superconductor. Unfortunately, a theory which applies to measurements carried out on dirty superconductors at high magnetic fields is not available at the present time. Moreover, there are only few published experimental data on the subject.<sup>5–7</sup> The purpose of this paper is twofold. First, to develop a phenomenological model for the magnetic-field variation of the ultrasonic attenuation in the mixed state ( $H_{c1} < H < H_{c2}$ ) of a high-field superconductor. Second, to present extensive experimental data on the attenuation in several high-field superconductors and to compare them in detail with the predictions of the model. It will be shown that the phenomenological model accounts quantitatively for the experimental results without the use of any adjustable parameters.

It has been pointed out by the present authors<sup>5,6</sup> that the salient features of the ultrasonic behavior of high-field superconductors arise from the strong influence

<sup>4</sup> R. W. Morse, in *Progress in Cryogenics*, edited by K. Mendelssohn (Heywood and Company, Ltd., London, 1959), Vol. I; D. H. Douglass, Jr., and L. M. Falicov, in *Progress in Low-Temperature Physics*, edited by C. J. Gorter (North-Holland Publishing Company, Amsterdam, 1964), Vol. IV, p. 97; N. Tepley, Proc. IEEE **53**, 1586 (1965); A. R. Mackintosh, *Phonons and Phonon Interactions* (W. A. Benjamin, Inc., New York, 1964), p. 181.

<sup>5</sup> Y. Shapira and L. J. Neuringer, Phys. Rev. Letters **15**, 724 (1965); Erratum, *ibid.* **15**, 873 (1965).

<sup>6</sup> L. J. Neuringer and Y. Shapira, Phys. Rev. **148**, 231 (1966).

<sup>7</sup> Y. Shapira and L. J. Neuringer, Phys. Rev. **140**, A1638 (1965).

\* Supported by the U. S. Air Force Office of Scientific Research.  
<sup>1</sup> Y. B. Kim, C. F. Hempstead, and A. R. Strnad, Phys. Rev. **139**, A1163 (1965).

<sup>2</sup> J. I. Gittleman and B. Rosenblum, Phys. Rev. Letters **16**, 734 (1966).

<sup>3</sup> B. Rosenblum and M. Cardona, Phys. Rev. Letters **12**, 657 (1964); B. Rosenblum, M. Cardona and G. Fischer, RCA Rev. **25**, 491 (1964); W. Hackett (to be published).

of the magnetic field on the ultrasonic attenuation and velocity. In particular, we have shown that the magnetic-field variation of the ultrasonic attenuation and velocity in the mixed and normal states of Nb-25 at.% Zr can be interpreted in terms of the Alpher-Rubin theory.<sup>8</sup> This theory was originally formulated to describe the effects of the magnetic field on the ultrasonic behavior of metals which are in the normal state. In our earlier study of Nb-25 at.% Zr we were unable, however, to account *quantitatively* for the ultrasonic results in the mixed state at frequencies above  $\sim 10$  Mc/sec. In Sec. II we develop a phenomenological model for the magnetic-field dependence of the ultrasonic attenuation in the mixed and normal states of high-field superconductors. This model is a natural generalization of our earlier treatment of the subject and takes into account, explicitly, the frequency dependence of the attenuation. It is shown that the attenuation in the mixed state depends markedly on the strength of the pinning forces which act on the flux lines. In particular, when the pinning forces are weak, or when the ultrasonic frequency is high, the attenuation is directly related to the dc flow resistance.

In Sec. III the physical properties of the specimens used in the present work are presented. In Sec. IV experimental data on the ultrasonic attenuation in five different high-field superconductors are presented and compared with predictions of the theoretical model. It is demonstrated that the ultrasonic attenuation in the mixed state depends on the strength of the pinning forces. A method for determining these forces from ultrasonic data is outlined and demonstrated. Finally, anomalies in the ultrasonic attenuation, which are probably related to the "peak effect"<sup>9</sup> in the critical current density, are discussed.

## II. THEORY

### A. General Considerations

The primary causes for ultrasonic attenuation in high-field superconductors subjected to intense magnetic fields are different from those responsible for the attenuation observed in pure type-I superconductors. This difference arises from the widely different physical properties of the two classes of materials, specifically the normal-state electrical resistivity and the magnitude of the superconducting-to-normal transition field.

It is well known<sup>4</sup> that the ultrasonic attenuation at zero magnetic field decreases rapidly when a metal becomes superconducting. If  $\alpha_n$  is the normal-state attenuation coefficient at *zero magnetic field*, then the attenuation coefficient  $\alpha_s$  in the superconducting state,

and at zero field, is given by

$$\alpha_s/\alpha_n = 2/[1 + \exp(\epsilon/kT)], \quad (1)$$

where  $2\epsilon$  is the temperature-dependent energy gap, and  $T$  is the absolute temperature. In studies of the ultrasonic attenuation in pure type-I superconductors, Eq. (1) is used to determine the energy gap. The fact that  $\alpha_n$  and  $\alpha_s$  refer to the attenuation coefficients *at zero field* can often be overlooked in these studies, since the magnetic fields which are used to quench the superconductivity are usually quite small ( $H \lesssim 1$  kG) and do not affect the attenuation coefficient significantly. Thus, it is a common procedure to apply a magnetic field  $H > H_{c2}$ , then measure the attenuation coefficient and assume that this attenuation coefficient is very nearly equal to  $\alpha_n$ . The situation in the case of high-field superconductors is radically different.

For metals with an electron mean free path which is short compared to the ultrasonic wavelength,  $\alpha_n$  is inversely proportional to the electrical resistivity. In general, high-field superconductors ( $H_{c2} \sim 100$  kG) have normal-state resistivities which are several orders of magnitude larger than those of typical pure type-I superconductors at low temperatures.<sup>9a</sup> Consequently,  $\alpha_n$  is much smaller in the case of high-field superconductors than in the case of pure type-I superconductors. On the other hand, the effects of a magnetic field on the ultrasonic attenuation, which can often be neglected in studying low-field superconductors, are quite large in the case of a high-field superconductor subjected to an intense magnetic field. This is true both in the mixed state and at fields above  $H_{c2}$ . For example, we have estimated<sup>6</sup> that for 10-Mc/sec shear waves in Nb-25 at.% Zr,  $\alpha_n$  is of the order of  $10^{-4}$  dB/cm. In the same material the observed attenuation change near  $H_{c2}$  ( $\sim 70$  kG) is  $\sim 0.6$  dB/cm at 4.2°K, which is accounted for, quantitatively, by considering the effects of the magnetic field on the attenuation.

The preceding arguments suggest that in discussing the ultrasonic attenuation in high-field superconductors which are subjected to strong magnetic fields, one may neglect  $\alpha_n$  (or the difference between  $\alpha_n$  and  $\alpha_s$ ) and consider only the effect of the magnetic field on the attenuation. This assumption is expected to be valid for ultrasonic frequencies in the 10-Mc range. At much higher frequencies  $\alpha_n$  can become comparable to, or larger than, the attenuation change caused by a magnetic field of  $\sim 10^4$ – $10^5$  G.

In earlier papers<sup>5,6</sup> we studied the ultrasonic behavior of Nb-25 at.% Zr in the mixed state and at  $H > H_{c2}$ . It was shown that the change with magnetic field of the ultrasonic attenuation and velocity can be understood in terms of the Alpher-Rubin theory,<sup>8</sup> which was originally derived for impure metals in the normal

<sup>8</sup> R. A. Alpher and R. J. Rubin, J. Acoust. Soc. Am. **26**, 452 (1954); hereafter referred to as AR.

<sup>9</sup> See S. H. Autler, E. S. Rosenblum, and K. H. Gooen, Phys. Rev. Letters **9**, 489 (1962); Rev. Mod. Phys. **36**, 77 (1964).

<sup>9a</sup> Few superconductors (e.g., V<sub>3</sub>Si) have a high upper critical field even when their normal-state resistivity is low. The present discussion may not apply to these exceptional materials.

state. It was found that the behavior of low-frequency (few Mc/sec) sound waves in the mixed state of Nb-25 at.% Zr follows the predictions of the Alpher-Rubin theory provided one assumes that the resistivity is zero. To interpret the results at higher frequencies it was necessary to assume the existence of a finite effective ac resistivity in the mixed state. It was argued that this effective ac resistivity has the same origin as the ordinary ac resistivity which was then being studied by Gittleman and Rosenblum.<sup>2</sup> In the present paper we shall continue to pursue this approach to the problem of ultrasonic attenuation in high-field superconductors. Specifically, we shall generalize the Alpher-Rubin theory by introducing a complex ac resistivity to describe the attenuation in the mixed state.

In Secs. II B-II D we consider the magnetic field variation of the ultrasonic attenuation in the mixed and normal states of a high-field superconductor ( $H_{c2} \sim 10^5$  G). We shall be concerned only with the effects of the magnetic field on the attenuation, and will neglect  $\alpha_n$  and the difference between  $\alpha_n$  and  $\alpha_s$ . Finally, we shall confine our attention to longitudinal waves propagating in a transverse magnetic field and to shear waves propagating in a parallel magnetic field.

### B. Attenuation in the Normal State ( $H > H_{c2}$ )

At fields above  $H_{c2}$  a high-field superconductor is in the normal state. The effects of a magnetic field on the ultrasonic attenuation are given in this case by the Alpher-Rubin (AR) theory, which has been extended by the present authors<sup>5,6</sup> to include the dependence of the attenuation on the angle between the applied magnetic field  $\mathbf{H}$  and the direction of propagation of the sound wave. Since the AR theory also serves as a basis for the discussion of ultrasonic attenuation in the mixed state, we shall review it briefly. A more complete discussion of this theory, and an account of experimental results in metals which are in the normal state, can be found elsewhere.<sup>5,6,10,11</sup>

The basic assumptions of the AR theory are:

(1) The equation of motion of the lattice in the presence of a magnetic field is

$$\frac{d^2 \xi}{dt^2} = -\frac{1}{d} \left[ \mathbf{F}_e + \frac{1}{c} (\mathbf{J} \times \mathbf{B}) \right], \quad (2)$$

where  $\xi$  is the displacement of the lattice,  $d$  is the density of the metal,  $\mathbf{J}$  is the current density associated with the sound wave,  $\mathbf{B}$  is the magnetic induction, and  $\mathbf{F}_e$  is the elastic force at zero field.  $\mathbf{F}_e$  can be expressed in terms of the Young's modulus  $Y$ , and the Poisson

ratio  $\nu$ , namely,

$$\mathbf{F}_e = \frac{Y}{2(1+\nu)} \left[ \nabla^2 \xi + \frac{1}{1-2\nu} \nabla(\nabla \cdot \xi) \right]. \quad (3)$$

(2) The current density  $\mathbf{J}$  is given by

$$\mathbf{J} = \sigma [\mathbf{E} + (1/c)(d\xi/dt \times \mathbf{B})], \quad (4)$$

where  $\sigma$  is the electrical conductivity and  $\mathbf{E}$  is the electric field associated with the sound wave.

Using the above assumptions together with Maxwell's equations one obtains the following relation between the frequency  $\omega$  and the propagation constant  $q$  of a small-amplitude longitudinal sound wave:

$$\omega^2 - V_l^2 q^2 = \frac{q^2 H^2 \mu \sin^2 \theta}{4\pi d(1 - ic^2 q^2 / 4\pi \sigma \mu \omega)}, \quad (5)$$

where  $V_l$  is the longitudinal sound velocity at zero field,  $\mu$  is the permeability of the metal, and  $\theta$  is the angle between  $\mathbf{H}$  and the propagation vector  $\mathbf{q}$  of the sound wave. The magnetic-field variation of the ultrasonic attenuation and velocity can be derived from Eq. (5). In this derivation we make the following approximations: (a) The term  $q^2$  which appears in the denominator of Eq. (5) is replaced by its zero-field value  $(\omega/V_l)^2$ . (b) In solving for  $q$ , terms which are proportional to the fourth power of  $H$ , or higher, are neglected. With these approximations it can be shown that the amplitude of the sound wave decays with the distance  $x$  as  $e^{-\alpha x}$ , where<sup>12</sup>

$$\alpha = \frac{\sigma \mu^2 H^2 \beta_l^2 \sin^2 \theta}{2dV_l c^2 (1 + \beta_l^2)} (\text{cm}^{-1}), \quad (6)$$

$$\beta_l = c^2 \omega / 4\pi \sigma \mu V_l^2. \quad (7)$$

The change  $\Delta V_l$  in the sound velocity is given by

$$\Delta V_l / V_l = \mu H^2 \sin^2 \theta / 8\pi d V_l^2 (1 + \beta_l^2). \quad (8)$$

For a shear wave the corresponding expressions are

$$\alpha = \frac{\sigma \mu^2 H^2 \beta_s^2 \cos^2 \theta}{2dV_s c^2 (1 + \beta_s^2)} (\text{cm}^{-1}), \quad (9)$$

$$\beta_s = c^2 \omega / 4\pi \sigma \mu V_s^2, \quad (10)$$

and

$$\Delta V_s / V_s = \mu H^2 \cos^2 \theta / 8\pi d V_s^2 (1 + \beta_s^2), \quad (11)$$

where  $V_s$  is the shear velocity at zero field.

In the present paper we shall specialize to the cases of a longitudinal wave propagating in a transverse magnetic field ( $\mathbf{q} \perp \mathbf{H}$ ) and of a shear wave propagating

<sup>10</sup> Y. Shapira and L. J. Neuringer, Phys. Letters **20**, 148 (1966).

<sup>11</sup> G. A. Alers and P. A. Fleury, Phys. Rev. **129**, 2425 (1963).

<sup>12</sup> The AR theory neglects the attenuation at zero magnetic field. Equation (6) therefore represents the change in the attenuation coefficient due to the magnetic field.

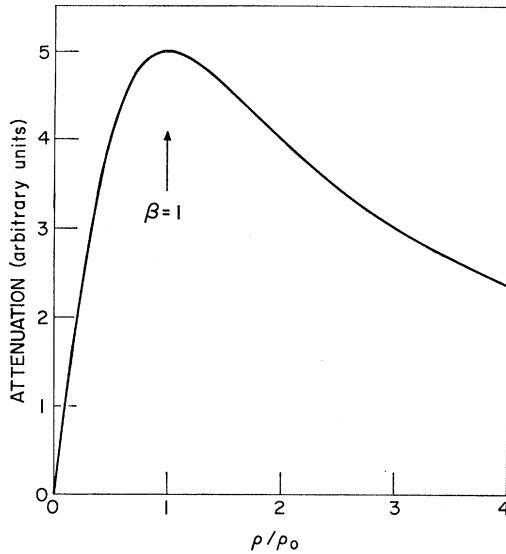


FIG. 1. Variation of the attenuation coefficient  $\alpha$  [Eqs. (12) and (13)] with the electrical resistivity  $\rho$ . It is assumed that the sample is in the normal state and that the magnetic field and ultrasonic frequency are fixed.

in a parallel magnetic field ( $\mathbf{q} \parallel \mathbf{H}$ ). As can be seen from Eqs. (6), (8), (9), and (11), the changes in attenuation and velocity are maximized (with respect to  $\theta$ ) at these configurations. The attenuation change due to the magnetic field can then be written as

$$\alpha = \left( \frac{\omega H^2 \mu}{8\pi d V^3} \right) \left( \frac{\beta}{1 + \beta^2} \right) (\text{cm}^{-1}), \quad (12)$$

$$\beta = c^2 \omega \rho / 4\pi \mu V^2 \equiv \rho / \rho_0, \quad (13)$$

where  $\rho$  is the electrical resistivity,

$$\rho_0 = 4\pi \mu V^2 / c^2 \omega, \quad (14)$$

and  $V$  is the sound velocity ( $V_l$  for a longitudinal wave, and  $V_s$  for a shear wave). Examination of Eqs. (12) and (13) indicates that  $\alpha$  is proportional to  $\omega^2$  at low frequencies ( $\beta \ll 1$ ) but is independent of  $\omega$  at high frequencies ( $\beta \gg 1$ ).

In studying the ultrasonic attenuation in high-field superconductors one is interested in the dependence of the attenuation on the electrical resistivity  $\rho$ . Equation (13) indicates that, at a given ultrasonic frequency, the parameter  $\beta$  is proportional to  $\rho$ . The dependence of  $\alpha$  on  $\rho$  is therefore given by the factor  $\beta/(1+\beta^2)$  which appears in Eq. (12). Hence, when  $\rho \ll \rho_0$ , the attenuation coefficient  $\alpha$  is proportional to  $\rho$ , but when  $\rho \gg \rho_0$ , the attenuation coefficient is inversely proportional to  $\rho$ . The variation of  $\alpha$  with  $\rho$  is shown in Fig. 1. It is seen that  $\alpha$  has a maximum with respect to  $\rho$  when  $\rho = \rho_0$ . At this maximum  $\beta = 1$ . Physically, the parameter  $\beta$  is related to the ratio of the classical

skin depth  $\delta$  and the ultrasonic wavelength  $\lambda$ :

$$\beta = 2\pi^2 (\delta/\lambda)^2. \quad (15)$$

The effect of the magnetic field on the attenuation of a sound wave of a given frequency is therefore largest when the electrical resistivity is such that  $\delta$  is comparable to  $\lambda$ . It is noteworthy that the resistivity  $\rho_0$  depends on the ultrasonic frequency. Consequently, with a given resistivity either of the conditions  $\rho \ll \rho_0$  and  $\rho \gg \rho_0$  can be achieved by varying  $\omega$ .

In concluding this review of the AR theory, it should be pointed out that this theory is valid only for metals with short electron mean free path, such as high-field superconducting alloys in the normal state.<sup>9a</sup> In this case one can show<sup>6</sup> that the more general expression for the variation of the ultrasonic attenuation with  $H$ , derived by Rodriguez,<sup>13</sup> reduces to Eqs. (12) and (13). On the other hand, when the electron mean free path is long, as is the case for pure metals at low temperatures, the AR theory is no longer valid.

### C. Extension of the AR Theory

The phenomenological model which we propose in order to describe the ultrasonic attenuation in the mixed state of a high-field superconductor is based on the AR theory. In this theory the metal in which the sound propagates is characterized, among other things, by its resistivity  $\rho$ . In their paper AR did not specify whether  $\rho$  is the dc or the ac resistivity. The distinction between the two types of resistivities is unimportant in the case of normal metals with short electron mean free path since the ac resistivity in the 10-Mc range is very close to the dc resistivity. This is not the case in the mixed state of type-II superconductors where the dc resistivity in the mixed state (at low current densities) is zero while the ac resistivity for sufficiently high frequencies differs from zero even at low current densities. Since the sound wave gives rise to ac currents, rather than to dc currents, it is natural to assume that the ultrasonic attenuation is determined by the ac resistivity.

It will be shown below that in the mixed state the ac resistivity is, in general, a complex quantity. The AR theory is generalized to include this case by assuming that the resistivity,  $\rho = \sigma^{-1}$ , which appears in Eq. (5), is a complex quantity. Instead of Eqs. (12) and (13) one then obtains

$$\alpha = \left( \frac{\omega H^2 \mu}{8\pi d V^3} \right) \left[ \frac{\beta_1}{(1 + \beta_2)^2 + \beta_1^2} \right] (\text{cm}^{-1}), \quad (16)$$

$$\beta_1 = \rho_1 / \rho_0, \quad (17a)$$

$$\beta_2 = \rho_2 / \rho_0, \quad (17b)$$

<sup>13</sup> S. Rodriguez, Phys. Rev. **130**, 1778 (1963).

where  $\rho_1$  and  $\rho_2$  are the real and imaginary parts of  $\rho$ , respectively. When  $\rho$  is real, these equations reduce to Eqs. (12) and (13).

In the case of high-field superconductors which are in the normal state ( $H > H_{c2}$ ) the ac resistivity is very nearly equal to the normal-state dc resistivity  $\rho_n$ , which is a real quantity. Also, the permeability  $\mu$  in the normal state is usually very nearly equal to unity. Therefore, the attenuation in the normal state is given by Eqs. (12) and (13) with  $\rho = \rho_n$  and  $\mu = 1$ .

#### D. Attenuation in the Mixed State

For a high-field superconductor which is in the mixed state, we shall assume that the magnetic-field variation of the attenuation is given by Eqs. (16) and (17), where  $\rho_1$  and  $\rho_2$  are the real and imaginary parts of the ac resistivity which are given below. We shall further assume that to a good approximation  $\mu = 1$  in the mixed state. The latter assumption is valid only when the magnetization of the sample is small compared to  $H$ , that is, when  $H \gg H_{c1}$ . However, since  $H_{c1}$  is usually of the order of 1 kG, whereas  $H_{c2} \sim 100$  kG, the approximation  $H \gg H_{c1}$  is satisfied in most of the mixed state.

A model for the ac resistivity in the mixed state has been developed by Gittleman and Rosenblum.<sup>2</sup> The following discussion is based on their model. We consider an ac electric current in the mixed state of a superconductor when the applied magnetic field is perpendicular to the current direction. The equation of motion of a flux line, for small displacements, is

$$m\ddot{x} + \eta\dot{x} + Kx = J\varphi_0/c, \quad (18)$$

where  $m$  is the effective mass of the flux line per unit length,  $x$  is the displacement of the flux line,  $\eta$  is a viscosity coefficient,  $Kx$  is the pinning force per unit length,  $J$  is the current density, and  $\varphi_0$  is the flux quantum  $hc/2e$ . The first term on the left-hand side of Eq. (18) is very small for frequencies in the 10-Mc range and will be neglected. Letting  $x = x_0 e^{i\omega t}$  and  $J = J_0 e^{i\omega t}$ , we obtain

$$x = J\varphi_0/c(i\omega\eta + K). \quad (19)$$

The electric field  $E$  is given by<sup>1</sup>

$$E = (\dot{x}/c)B = i\omega BJ\varphi_0/c^2(i\omega\eta + K). \quad (20)$$

From Eqs. (19) and (20) one obtains the ac resistivity

$$\rho = E/J = i\omega B\varphi_0/c^2(i\omega\eta + K). \quad (21)$$

Hence

$$\rho_1 = \omega^2\eta B\varphi_0/c^2(\omega^2\eta^2 + K^2), \quad (22a)$$

and

$$\rho_2 = \omega KB\varphi_0/c^2(\omega^2\eta^2 + K^2). \quad (22b)$$

The viscosity coefficient  $\eta$  is given by the expression<sup>1</sup>

$$\eta = \varphi_0 H_{c2}^*(0)/\rho_n c^2, \quad (23)$$

where  $H_{c2}^*(0)$  is the Ginzburg-Landau-Abrikosov-Gor'kov (GLAG) upper critical field at zero tempera-

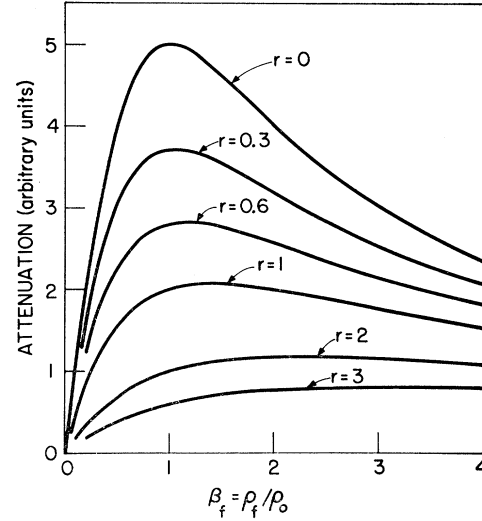


Fig. 2. Variation of the attenuation coefficient  $\alpha$  in the mixed state [Eq. (28)] with the flow resistivity  $\rho_f$ . The magnetic field is taken to be constant. The various curves are for different values of the parameter  $r = \omega_0/\omega$ .

ture.<sup>14</sup> From Eqs. (22) and (23) we have

$$\rho_1 = B\rho_n/H_{c2}^*(0)(1+r^2), \quad (24a)$$

$$\rho_2 = rB\rho_n/H_{c2}^*(0)(1+r^2), \quad (24b)$$

where

$$r = K/\eta\omega \equiv \omega_0/\omega. \quad (25)$$

The frequency  $\omega_0 = K/\eta$  at which the pinning force has the same magnitude as the viscous force will be called the depinning frequency. At fields  $H \gg H_{c1}$  the magnetic induction  $B$  is very nearly equal to  $H$ . Equations (24) can then be written as

$$\rho_1 = \rho_f/(1+r^2), \quad (26a)$$

$$\rho_2 = r\rho_f/(1+r^2), \quad (26b)$$

where

$$\rho_f = \rho_n H/H_{c2}^*(0) \quad (27)$$

is the dc flow resistivity.<sup>1</sup> Equations (16), (17), and (26) yield the following expression for the attenuation coefficient in the mixed state at  $H \gg H_{c1}$ :

$$\alpha = \left( \frac{\omega H^2 \mu}{8\pi d V^3} \right) \frac{\beta_f(1+r^2)}{[(1+r^2+r\beta_f)^2 + \beta_f^2]} (\text{cm}^{-1}), \quad (28)$$

where  $\beta_f = \rho_f/\rho_0$ . It can be shown that  $\alpha$  always decreases whenever  $\omega_0$  (and hence  $r$ ) increases. Thus, an increase in the pinning forces causes a decrease in the attenuation. The dependence of  $\alpha$ , for a given  $H$  and  $\omega$ , on  $\beta_f$  and  $r$  is shown in Fig. 2.

<sup>14</sup> In some cases  $H_{c2}^*(0)$  is higher than the actual upper critical field at zero temperature  $H_{c2}(0)$ . See, for example, L. J. Neuringer and Y. Shapira, Phys. Rev. Letters **17**, 81 (1966), and references therein.

TABLE I. Physical properties of the specimens.

| Nominal composition        | Annealing temperature (°C) | Density at 4.2°K $d$ (g/cm <sup>3</sup> ) | dc resistivity <sup>a</sup> $\rho_n$ ( $\mu\Omega$ cm) | Shear <sup>b</sup> velocity $V_s$ (10 <sup>6</sup> cm/sec) | Longitudinal <sup>b</sup> velocity $V_l$ (10 <sup>6</sup> cm/sec) | $H_{c2}^*(0)$ [Eq. (29)] (kG) | $H_{c2}^*(0)$ [Eq. (30)] (kG) | $J_c$ at 40 kG <sup>c</sup> (A/cm <sup>2</sup> ) | $\nu_0 = \omega_0/2\pi$ at 40 kG <sup>c</sup> (Mc/sec) |
|----------------------------|----------------------------|---|--|--|---|-------------------------------|-------------------------------|--|--|
| Nb-25 at.% Zr (unannealed) | unannealed                 | 8.1                                       | 27.5   | 1.88   | 4.7   | 87.8                          | 85.6                          | $4.0 \times 10^3$                                | 56   |
| Nb-25 at.% Zr (annealed)   | unknown                    | 8.1                                       | 26   | 1.97   | ...   | 83                            | ...                           | $8.0 \times 10^2$                                | 11   |
| Nb-32 at.% Ti              | 1300                       | 7.3                                       | 33.6   | 2.11   | 5.04  | ...                           | 102                           | $1.1 \times 10^3$                                | 1.6  |
| V-42 at.% Ti               | 1200                       | 5.4                                       | 59   | 2.6  | 5.6   | 161                           | 153                           | 50   | 0.8  |
| V-21 at.% Ti               | 1200                       | 5.7                                       | 29.6   | 2.71   | 5.9   | 77.5                          | ...                           | $5.0 \times 10^2$                                | 8.4  |

<sup>a</sup> Measured at 4.2°K and at  $H > H_{c2}$ .

<sup>b</sup> Measured at 4.2°K.

<sup>c</sup> Values are for 4.2°K, except for V-21 at.% Ti, where the value is for 1.5°K.

There are few limiting cases in which Eq. (28) simplifies considerably. When  $\omega$  tends to zero, or when the depinning frequency tends to infinity, the attenuation coefficient  $\alpha$  tends to zero. Thus, in the limit of very strong pinning forces the attenuation in the mixed state, at  $H \gg H_{c1}$ , does not vary with  $H$ . In the other extreme case the pinning forces are weak; i.e., when  $r \ll 1$ , Eq. (28) reduces to Eq. (12) with  $\beta_f$  replacing  $\beta$ . In other words, when the ultrasonic frequency  $\omega$  is much higher than the depinning frequency  $\omega_0$ , the magnetic-field variation of the attenuation in the mixed state can be obtained from the expression for the attenuation in the normal state [Eqs. (12) and (13)] by replacing the resistivity  $\rho$  by the flow resistivity  $\rho_f(H)$ . It should be noted that while  $\rho_f$  is always smaller than  $\rho_n$ , the attenuation calculated from Eqs. (12) and (13) with  $\rho = \rho_f$  may be larger than that calculated with  $\rho = \rho_n$ .

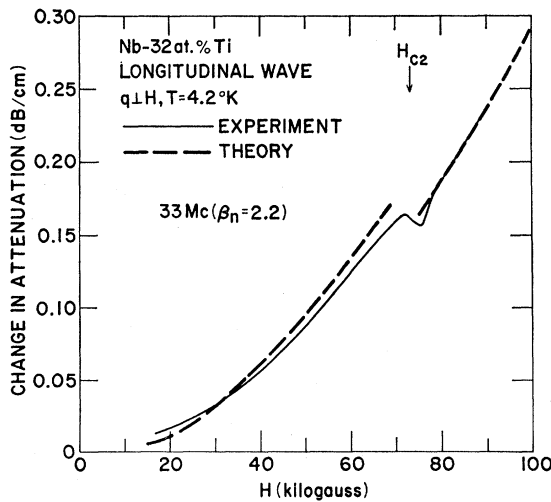


FIG. 3. Magnetic-field variation of the attenuation of 33-Mc/sec longitudinal waves in Nb-32 at.% Ti at 4.2°K. The magnetic field is perpendicular to the direction of sound propagation. The dashed curve is calculated from Eqs. (12) and (13) with  $\rho = \rho_f$  at  $H < H_{c2}$  and  $\rho = \rho_n$  at  $H > H_{c2}$ . The experimental and theoretical curves coincide at  $H > H_{c2}$ .

This may happen when the parameter  $\beta$  in the normal state is greater than unity (Fig. 1). As a consequence, the attenuation coefficient  $\alpha$  in the mixed state can be larger, over a certain magnetic-field interval, than it would have been had the material been normal.

To calculate  $\rho_f$  it is necessary to know the GLAG upper critical field at zero temperature  $H_{c2}^*(0)$ . This field may be obtained from the expression<sup>1,14</sup>

$$H_{c2}^*(0) = 3.1 \times 10^4 \rho_n \gamma T_c \text{ G}, \quad (29)$$

where  $\gamma$  is the electronic-specific-heat coefficient of the normal state in  $\text{erg cm}^{-3} \text{ deg}^{-2}$ ,  $T_c$  is the transition temperature in °K, and  $\rho_n$  is in  $\Omega$  cm. Alternatively,  $H_{c2}^*(0)$  may be determined from the measured upper critical field  $H_{c2}(T)$  via the relation<sup>14</sup>

$$H_{c2}^*(0) = -0.69 T_c (dH_{c2}/dT)_{T=T_c}. \quad (30)$$

The depinning frequency  $\omega_0$  plays a central role in the discussion of the ultrasonic attenuation in the mixed state. In order to obtain a meaningful comparison between theory and experiment, it is necessary to obtain an estimate of this frequency. Following Gittleman and Rosenblum<sup>2</sup> we assume that the pinning force constant  $K$  may be estimated from the critical current density  $J_c$  in the following way. For a small displacement of a flux line, the pinning force per unit length,  $F_p$ , is equal to  $Kx$ . For an arbitrary displacement, it is assumed that

$$F_p = (1/2\pi) s K \sin(2\pi x/s), \quad (31)$$

where  $s$  is the spacing between adjacent flux lines. It is further assumed that the maximum of the pinning force is equal to the Lorentz force at the critical current density  $J_c$ , i.e.,

$$sK/2\pi = J_c \phi_0 / c. \quad (32)$$

Hence

$$\omega_0 = 2\pi J_c \rho_n c / s H_{c2}^*(0). \quad (33)$$

When  $H \gg H_{c1}$ , the spacing between flux lines is given

by the relation<sup>15</sup>

$$\varphi_0/s^2 \approx H. \quad (34)$$

Substituting Eq. (34) into (33) we obtain

$$\omega_0 \approx 2\pi J_c \rho_n c H^{1/2} / \varphi_0^{1/2} H_{c2}^*(0). \quad (35)$$

Equation (35) should be regarded as a means of obtaining a *rough estimate*, rather than an exact value, of  $\omega_0$ . In addition, there are some experimental data which suggest that the pinning force constant  $K$  (and hence  $\omega_0$ ) for shear waves propagating in a parallel magnetic field differs somewhat from the one for longitudinal waves in a perpendicular field. This is not too surprising since the type of distortion which the flux lines undergo in the presence of a shear wave is expected to differ from the one involved in the case of a longitudinal wave.

### III. PHYSICAL PROPERTIES OF THE SPECIMENS

Experiments were performed on annealed superconducting alloys with the following nominal compositions: Nb-25 at.% Zr, Nb-32 at.% Ti, V-42 at.% Ti, and V-21 at.% Ti. These samples were annealed in vacuum ( $\sim 10^{-6}$  mm Hg) for 16 h at the temperatures which are listed in Table I. In addition, experiments were also carried out on an unannealed sample of Nb-25 at.% Zr.

Direct-current resistance measurements were performed on bars, cut from each of the superconducting alloys, using a four-probe technique. The normal-state resistivities at 4.2°K ( $H > H_{c2}$ ) are listed in Table I. No magnetoresistance was observed in the normal state. The superconducting-to-normal resistive transitions were measured at several temperatures with  $\mathbf{H}$  perpendicular to the applied current. For a given current density  $J$  the field  $H_r(J)$  at which the resistance was equal to half the normal resistance was found to decrease with increasing  $J$ . The resistive transition field at zero current,  $H_r(0)$ , was obtained by extrapolating  $H_r(J)$  to zero current. We chose to identify  $H_r(0)$  with the upper critical field  $H_{c2}$ .<sup>16</sup> Some values of  $H_{c2}$  are shown in Figs. 3-9.

The GLAG upper critical field at zero temperature  $H_{c2}^*(0)$  was determined by one or both of the procedures discussed in Sec. IID. For the Nb-Zr and Ti-V alloys the known values of  $\gamma$ <sup>17</sup> together with the measured values of  $\rho_n$  and  $T_c$  were used to determine  $H_{c2}^*(0)$  [Eq. (29)]. In the cases of Nb-32 at.% Ti, V-42 at.% Ti, and the unannealed Nb-25 at.% Zr,  $H_{c2}^*(0)$  was determined from Eq. (30) using the measured temperature variation of  $H_{c2}$ . Values of  $H_{c2}^*(0)$  are listed in Table I.

<sup>15</sup> P. G. de Gennes, *Superconductivity of Metals and Alloys* (W. A. Benjamin, Inc., New York, 1966), Chap. 3.

<sup>16</sup> This choice is somewhat arbitrary inasmuch as the resistive transition has a finite width. However, since the resistive transitions were rather sharp ( $\sim 2$ -5 kG wide), the error introduced by identifying  $H_r(0)$  with  $H_{c2}$  is small.

<sup>17</sup> A. El Bindari and M. M. Litvak, *J. Appl. Phys.* **34**, 2913 (1963); C. H. Cheng, K. P. Gupta, E. C. Van Reuth, and P. A. Beck, *Phys. Rev.* **126**, 2030 (1962).

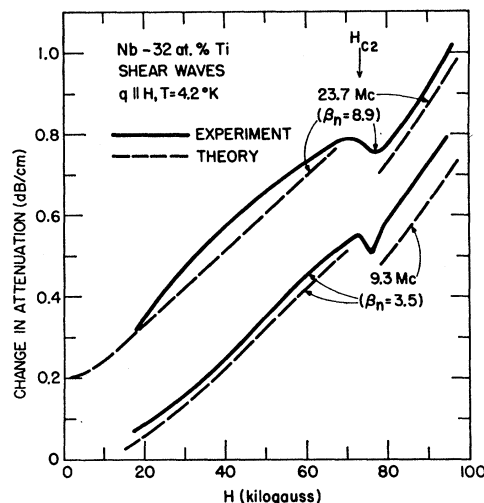


FIG. 4. Magnetic-field variation of the attenuation of shear waves in Nb-32 at.% Ti at 4.2°K. The magnetic field is parallel to the direction of sound propagation. The dashed curves are calculated from Eqs. (12) and (13) with  $\rho = \rho_f$  at  $H < H_{c2}$  and  $\rho = \rho_n$  at  $H > H_{c2}$ . The curves for the 23.7-Mc/sec wave are shifted upward by 0.2 dB/cm.

The critical current density  $J_c$  was measured at several temperatures. The applied magnetic field was normal to the direction of current flow. Values of  $J_c$  at 40 kG are listed in Table I. Using these values and Eq. (35), the depinning frequency  $\omega_0$  was estimated. Values of the frequency  $\nu_0 = \omega_0/2\pi$  at 40 kG, obtained in this fashion, are given in Table I. Also listed in Table I are the sound velocities which were measured by standard pulse techniques. The uncertainty in the velocity measurements is  $\pm 2\%$ .

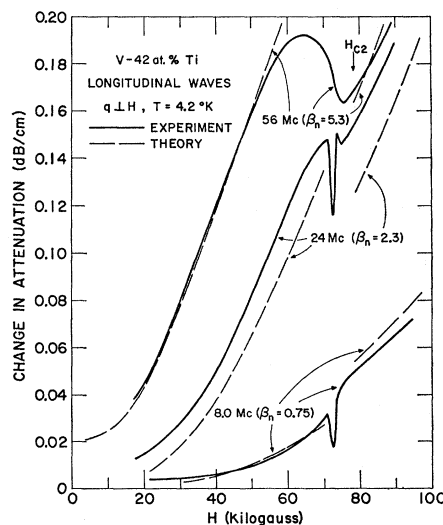


FIG. 5. Magnetic-field variation of the attenuation of longitudinal waves in V-42 at.% Ti at 4.2°K. The dashed curves are calculated from Eqs. (12) and (13) with  $\rho = \rho_f$  at  $H < H_{c2}$  and  $\rho = \rho_n$  at  $H > H_{c2}$ . The curves for the 56-Mc/sec wave are shifted upward by 0.02 dB/cm.

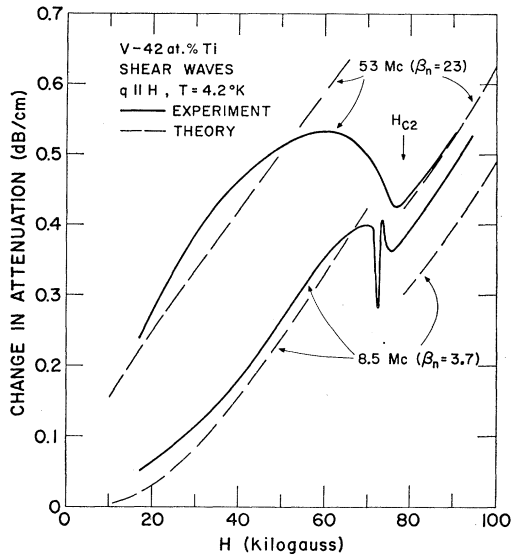


FIG. 6. Magnetic-field variation of the attenuation of shear waves in V-42 at.% Ti at 4.2°K. The dashed curves are calculated from Eqs. (12) and (13) with  $\rho = \rho_f$  at  $H < H_{c2}$  and  $\rho = \rho_n$  at  $H > H_{c2}$ . The curves for the 53-Mc/sec wave are shifted upward by 0.1 dB/cm.

#### IV. RESULTS AND DISCUSSION

Ultrasonic-attenuation measurements were carried out on the five superconducting alloys at liquid-helium temperatures and in steady magnetic fields up to 100 kG. In the case of the Nb-Zr alloys the ultrasonic specimens were cylindrically shaped, about 0.7-in. long, and 0.26-in. in diam. The other ultrasonic specimens were cubes with an edge about 0.4-in. long. Acoustical bonds were made with Dow Corning 200 silicone oil having a viscosity of 30 000 centistoke at 25°C. The variation of the ultrasonic attenuation with  $H$  was measured by the pulse-echo technique using a procedure which has previously been described.<sup>6,18</sup> The accuracy of the attenuation measurements is estimated to be better than 10% for  $\sim 10$ -Mc/sec waves, and is somewhat poorer at higher frequencies ( $\sim 15\%$  at 50 Mc/sec).

The discussion of the ultrasonic data is divided into several parts. In Secs. IV A–IV C we discuss the results in the mixed and normal states. We start with the case in which the pinning forces in the mixed state are very weak, then turn to the case in which the pinning forces are very strong, and conclude with the case in which the pinning forces are comparable to the viscous forces ( $\omega$  is of the order of  $\omega_0$ ). In Sec. IV D we discuss the ultrasonic behavior at fields just below  $H_{c2}$ , where certain anomalies in the ultrasonic attenuation occur. These anomalies are believed to be associated with the “peak effect.”

<sup>18</sup> Y. Shapira and B. Lax, Phys. Rev. **138**, A1191 (1965).

#### A. Weak Pinning Forces ( $\omega_0 \ll \omega$ )

The superconducting alloys V-42 at.% Ti and Nb-32 at.% Ti, which were studied in the present experiments, have very weak pinning forces. The estimated depinning frequencies in these materials are less than 2 Mc/sec (Table I). From the arguments of Sec. II one expects that for sound waves in the 10-Mc range the magnetic-field variation of the attenuation in the mixed state would follow Eqs. (12) and (13) with  $\rho = \rho_f$ , whereas in the normal state the attenuation should obey these equations with  $\rho = \rho_n$ . The results of ultrasonic-attenuation measurements in these two alloys, together with the predictions of the theory, are shown in Figs. 3–6. The theoretical curves were calculated using the parameters which are listed in Table I.<sup>19</sup> As can be seen, there is good agreement between the experimental results and the theoretical calculations. The only significant difference between experiment and theory occurs for  $\sim 50$ -Mc/sec waves in V-42 at.% Ti where at fields close to  $H_{c2}$  the observed attenuation is smaller than the one predicted by the theory. This discrepancy is probably related to the fact that the flow resistivity, as determined by dc resistive measurements, also deviates in many cases from Eq. (27) at fields close to  $H_{c2}$ .<sup>1</sup>

It is interesting to examine in greater detail the magnetic-field variation of the attenuation in the

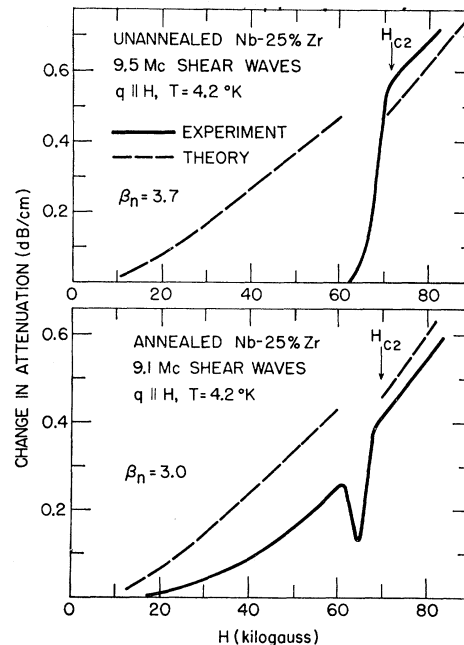


FIG. 7. Magnetic-field variation of the attenuation of shear waves in unannealed and annealed Nb-25 at.% Zr at 4.2°K. The dashed curves are calculated from Eqs. (12) and (13) with  $\rho = \rho_f$  for  $H < H_{c2}$  and  $\rho = \rho_n$  at  $H > H_{c2}$ .

<sup>19</sup> For V-42 at. % Ti we have let  $H_{c2}^*(0) = 157$  kG, which is the average of the two values given in Table I.



mixed state when the pinning forces are weak. The attenuation is expected to follow Eqs. (12) and (13) with  $\rho = \rho_f$ . Consider first the case when the parameter  $\beta$  in the normal state,  $\beta_n$ , is smaller than unity. Since  $\rho_f < \rho_n$ , the attenuation in the mixed state, at a given magnetic field, should be smaller than the attenuation which would have been present had the material been normal (Fig. 1). This is illustrated by the case of the 8-Mc/sec longitudinal wave propagating in V-42 at. % Ti (Fig. 5). On the other hand, consider the situation when  $\beta_n > 1$ . The ac resistivity in the mixed state  $\rho \approx \rho_f$  is smaller than  $\rho_n$ . However, as can be seen from Fig. 1, the attenuation at a given magnetic field may be higher for  $\rho = \rho_f$  than for  $\rho = \rho_n$ . Therefore, over a certain magnetic-field interval the attenuation in the mixed state can be higher than the attenuation which would have been present had the material been normal. This point is illustrated by the results for 56-Mc/sec longitudinal waves and 53-Mc/sec shear waves in V-42 at. % Ti, as well as by the results for 23.7-Mc/sec shear waves in Nb-32 at. % Ti.

Finally, it should be emphasized that all the theoretical curves for the magnetic-field variation of the ultrasonic attenuation do not contain any adjustable parameters. In view of this fact, we consider the agreement between theory and experiment as quite satisfactory.

**B. Strong Pinning Forces ( $\omega_0 \gg \omega$ )**

Among the superconductors investigated in the present work the *unannealed* Nb-25 at. % Zr alloy has the highest depinning frequency ( $\nu_0 \approx 56$  Mc/sec at 40 kG). In this material one expects that the pinning forces would be much stronger than the viscous forces

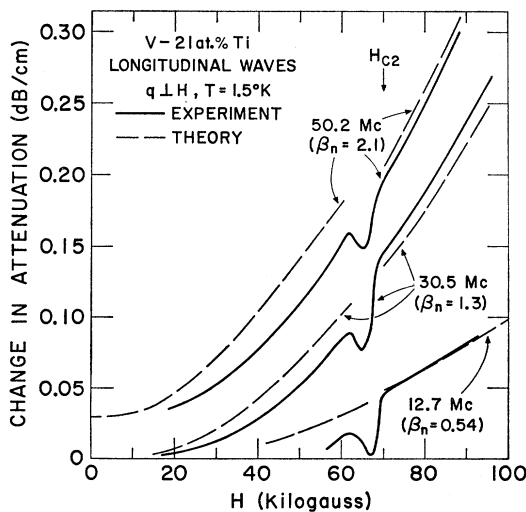


FIG. 8. Magnetic-field variation of the attenuation of longitudinal waves in V-21 at. % Ti at 1.5°K. The dashed curves are calculated from Eqs. (12) and (13) with  $\rho = \rho_f$  at  $H < H_{c2}$  and  $\rho = \rho_n$  at  $H > H_{c2}$ . The curves for the 50.2-Mc/sec wave are shifted upward by 0.03 dB/cm.

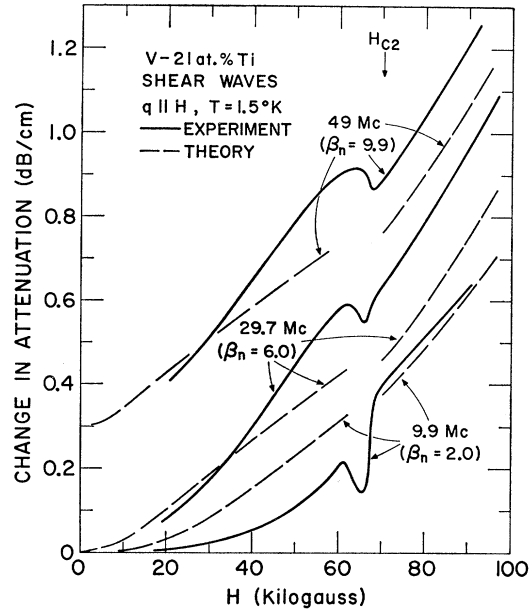


FIG. 9. Magnetic-field variation of the attenuation of shear waves in V-21 at. % Ti at 1.5°K. The dashed curves are calculated from Eqs. (12) and (13) with  $\rho = \rho_f$  at  $H < H_{c2}$ , and  $\rho = \rho_n$  at  $H > H_{c2}$ . The curves for the 49-Mc/sec wave are shifted upward by 0.3 dB/cm.

at frequencies in the megacycle range. As a consequence, the magnetic-field variation of the attenuation in the mixed state should be substantially smaller than that predicted by Eqs. (12) and (13) with  $\rho = \rho_f$ . To test this prediction we have measured the attenuation of 5- and 9.5-Mc/sec shear waves propagating in a parallel magnetic field at 4.2°K. As expected, the attenuation was found to be almost independent of  $H$  at  $H < H_{c2}$ . The results for the 9.5-Mc/sec shear wave are shown in the upper part of Fig. 7. It is seen that at  $H < H_{c2}$  there is no observable change of the attenuation with  $H$ . In the normal state ( $H > H_{c2}$ ) the attenuation is in good agreement with that calculated from Eqs. (12) and (13) with  $\rho = \rho_n$ .

The absence of observable change in the attenuation of 9.5-Mc/sec shear waves in the mixed state of unannealed Nb-25 at. % Zr was attributed to the presence of strong pinning forces. To test this explanation we have measured the attenuation of 9.1-Mc/sec shear waves in an annealed specimen of Nb-25 at. % Zr. As in the case of the unannealed sample, the magnetic field was along the direction of sound propagation and the temperature was 4.2°K. The results are shown in the bottom half of Fig. 7. In the annealed specimen the pinning forces are much weaker than in the unannealed sample (Table I). One therefore expects an observable magnetic-field variation of the attenuation in the mixed state, and this is precisely what is observed.

For the unannealed Nb-25 at. % Zr,  $\omega_0 \gg \omega$  for frequencies in the megacycle range. However, by increasing the ultrasonic frequency it should be possible to

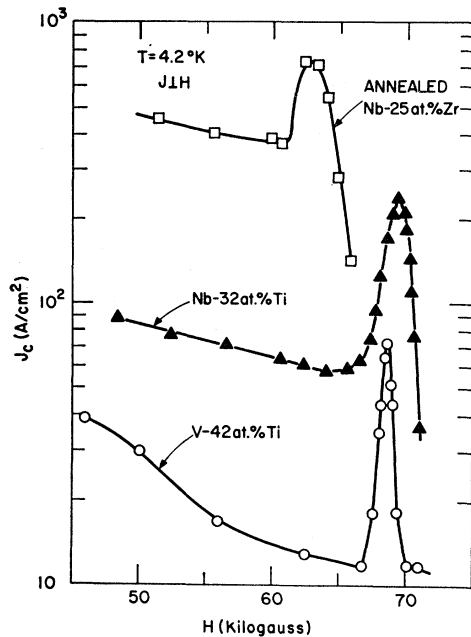


FIG. 10. Critical current density as a function of  $H$  for annealed Nb-25 at.% Zr, Nb-32 at.% Ti, and V-42 at.% Ti at 4.2°K. Note the "peak effect" in all three samples.

decrease the parameter  $r = \omega_0/\omega$  with the result that the attenuation would vary considerably with  $H$  at  $H < H_{c2}$ . The observation of such magnetic-field-dependent attenuation (in the mixed state of the same sample) at frequencies above  $\sim 25$  Mc/sec has already been reported by the authors.<sup>5,6</sup>

### C. Pinning Forces Comparable to Viscous Forces

$$(\omega_0 \sim \omega)$$

In Secs. IV A and IV B we considered situations in which the pinning forces are either very weak ( $\omega_0 \ll \omega$ ) or very strong ( $\omega_0 \gg \omega$ ). We turn now to the case in which  $\omega$  is comparable to  $\omega_0$ . Under this condition a non-negligible ac resistance should exist in the mixed state, resulting in a noticeable magnetic-field variation of the attenuation at  $H < H_{c2}$ . However, this variation should be smaller than that predicted by Eqs. (12) and (13) with  $\rho = \rho_f$  (Fig. 2).

The superconducting alloys V-21 at.% Ti and annealed Nb-25 at.% Zr have depinning frequencies of the order of  $\sim 10$  Mc/sec (Table I). One therefore expects that the predictions of the preceding paragraph would hold for  $\sim 10$ -Mc/sec sound waves propagating in these alloys. Examination of Figs. 7, 8, and 9 shows that this is, in fact, the case.

The dependence of the attenuation in the mixed state on  $\omega_0$  enables one to estimate the depinning frequency from ultrasonic data. To demonstrate the procedure we estimate the depinning frequencies in V-21 at.% Ti and annealed Nb-25 at.% Zr from the attenuation curves in Figs. 7 and 9. For the 9.1-Mc/sec

shear wave in annealed Nb-25 at.% Zr the observed attenuation at 40 kG is equal to 0.36 times the attenuation calculated from Eqs. (12) and (13) with  $\rho = \rho_f$ . Also at this field  $\beta_f = 1.47$ . Using Fig. 2 we estimate  $r = \omega_0/\omega \approx 1.4$ . This gives  $\nu_0 \approx 13$  Mc/sec at 40 kG. Similarly, from the results for 9.9-Mc/sec shear waves in V-21 at.% Ti we estimate  $\nu_0 \approx 12$  Mc/sec at 40 kG. These estimates are in good agreement with the values given in Table I, which were calculated from Eq. (35) using the measured critical current densities.

In the superconducting alloy V-21 at.% Ti we expect the inequality  $\omega \gg \omega_0$  to hold at  $\sim 50$  Mc/sec. Consequently, at this frequency the magnetic-field variation of the ultrasonic attenuation in the mixed state should follow Eqs. (12) and (13) with  $\rho = \rho_f$ . Examination of Figs. 8 and 9 shows that the attenuation curves for 50.2-Mc/sec longitudinal waves and 49-Mc/sec shear waves are reasonably well represented by the theoretical curves with  $\rho = \rho_f$ . The agreement for the shear waves is, however, not as good as in the cases of V-42 at.% Ti and Nb-32 at.% Ti, for which materials the inequality  $\omega \gg \omega_0$  is better satisfied at 50 Mc/sec.

### D. Attenuation Dips Near $H_{c2}$

Examination of Figs. 5-9 shows that in many cases the attenuation has a sharp dip at  $H \approx H_{c2}$ . This type of attenuation dip was first observed by the present authors in Nb-Ti alloys.<sup>7</sup> We believe that this anomalous behavior of the ultrasonic attenuation is related to the "peak effect" in the critical current density.

It is well known<sup>9</sup> that in many type-II superconductors the critical current density  $J_c$  as a function of  $H$  exhibits a peak at a field which is slightly below  $H_{c2}$ . This phenomenon, which is called the "peak effect," has been observed in all the annealed specimens used in the present work. Figure 10 shows the peak effect in some of the alloys. The influence of the peak effect on the ultrasonic attenuation can be understood qualitatively in terms of the discussion of Sec. II. The sharp increase in  $J_c$  corresponds to an increase of the pinning forces and should result in a sharp decrease in the ultrasonic attenuation. Examination of the attenuation curves in Figs. 5-9 shows that the field at which the attenuation dip occurs is close to the field where the critical current density exhibits a sharp maximum.<sup>20</sup>

The arguments of Sec. II indicate that when  $\omega \gg \omega_0$ , the attenuation is independent of the pinning forces. It is therefore expected that even though the pinning forces increase sharply when the peak effect occurs, the ultrasonic attenuation will not be affected appreciably provided the ultrasonic frequency is sufficiently high. This prediction is borne out by the attenuation curves for V-42 at.% Ti (Figs. 5 and 6), where, at frequencies of

<sup>20</sup> The slight difference between the field at which the attenuation exhibits a dip and the field at which the peak effect occurs is probably related to the fact that the bars used in the critical-current measurements and the ultrasonic samples were cut from different portions of the original specimens.

$\sim 8$  and 24 Mc/sec the attenuation exhibits a sharp dip, whereas the attenuation of  $\sim 50$ -Mc/sec waves varies smoothly with  $H$  near  $H_{c2}$ .

## V. CONCLUSION

The experimental results presented in this paper indicate that the phenomenological model (Sec. II) accounts quantitatively for the ultrasonic attenuation in high-field superconductors. It therefore appears that while a rigorous microscopic theory for the ultrasonic behavior of high-field superconductors does not exist at the present time, one can obtain a good description of the ultrasonic attenuation in the mixed and normal states by using the phenomenological model.

It was shown that the ultrasonic attenuation in the mixed state is related to the motion of the flux lines and is markedly affected by the strength of the pinning forces which inhibit this motion. In particular, when the ultrasonic frequency is high compared to the depinning frequency, the attenuation is directly related to the dc flow resistance. A method of obtaining an

estimate of the depinning frequency, and hence the strength of the pinning forces, from ultrasonic attenuation measurements was outlined and demonstrated.

Finally, it should be noted that although we have restricted ourselves to the discussion of the ultrasonic *attenuation*, one should be able to use the same phenomenological approach to describe the magnetic-field variation of the ultrasonic *velocity* in high-field superconductors.<sup>21</sup>

## ACKNOWLEDGMENTS

We are grateful to J. K. Hulm and W. T. Reynolds of the Westinghouse Research Laboratories for providing the samples used in this study. We also wish to thank M. Kelly for technical assistance.

<sup>21</sup> The equation for the magnetic-field variation of the sound velocity in the mixed state and at  $H \gg H_{c1}$  is

$$\frac{\Delta V}{V} = \frac{\mu H^2}{8\pi d V^2} \left[ \frac{(1+r^2+r\beta_f)(1+r^2)}{(1+r^2+r\beta_f)^2 + \beta_f^2} \right]$$

This expression should hold for longitudinal waves with  $\mathbf{q} \perp \mathbf{H}$ , and for shear waves with  $\mathbf{q} \parallel \mathbf{H}$ . The magnetic-field variation of the shear velocity in unannealed Nb-25 at.% Zr (Refs. 5, 6) is in agreement with the above equation.

## Possible Non-One-Electron Effects in the Fundamental Optical Excitation Spectra of Certain Crystalline Solids and Their Effect on Photoemission\*

WILLIAM E. SPICER

*Stanford Electronics Laboratories, Stanford University, Stanford, California*

(Received 16 May 1966; revised manuscript received 30 September 1966)

Intrinsic optical excitation in solids is considered for the case where localization of the hole or electron is important. It is noted that Koopmans's theorem (or the quasiparticle description) will not in general hold in such a case; as a result the optical excitation must be considered in terms of a many-body excitation rather than in the one-electron (or quasiparticle) approximation. The many-body effects are considered qualitatively in terms of the relaxation about a "localized hole" for two extreme cases. The first of these is that in which the relaxation is electronic in nature and takes place in a time comparable to the excitation time. The second is that in which the relaxation is ionic in nature and takes place after the optical excitation event.

## I. INTRODUCTION

TO date most of the interpretation of the intrinsic optical spectra of solids has been based on the use of the one-electron band approximation and on the assumption that Koopmans's theorem<sup>1,2</sup> applies. Except in

\* This work was supported by the U. S. Advanced Research Projects Agency through the Center for Materials Research at Stanford University and by the National Science Foundation grant NSF-GK-149, the National Aeronautics and Space Administration grant NGR-05-020-066, the U. S. Army Research Office, Durham, contract DA-31-124-ARO-D-430, and the U. S. Army Night Vision Laboratory, Fort Belvoir, contract DA-44-009-AMC-1474(T).

<sup>1</sup> Koopmans's theorem states that the one-electron energy eigenvalue  $\epsilon_j$  in the Fock equation for a solid is the negative of the energy to remove the electron in state  $\varphi_j$  from the solid. The proof of Koopmans's theorem depends on the spatial part of the wave function being of the Bloch type and on all other wave functions being unchanged when one electron is removed. If Koopmans's

theorem holds, it follows that the photon energy necessary to excite an electron from state  $\varphi_i$  to state  $\varphi_k$  is just the difference between the one electron energies of the two states. However, if the eigenfunctions of other states are modified in the excitation, Koopmans's theorem will not hold, and many-body effects must be taken into account.

<sup>2</sup> F. Seitz, *Modern Theory of Solids* (McGraw-Hill Book Company, Inc., New York, 1940), p. 313; J. Callaway, *Energy Band Theory* (Academic Press Inc., New York, 1964), p. 117; J. C. Phillips, *Phys. Rev.* **123**, 420 (1961).

<sup>3</sup> The author considers Phillips's resonance (Refs. 5 and 32) and Hopfield's electron-electron interaction studies (Ref. 57) to be notable exceptions.

<sup>4</sup> L. G. Parratt, *Rev. Mod. Phys.* **31**, 616 (1959).